



Amelioration of the nigrostriatal pathway facilitated by ultrasound-mediated neurotrophic delivery in early Parkinson's disease

Maria Eleni Karakatsani^{a,1}, Shutao Wang^{a,1}, Gesthimani Samiotaki^{a,1}, Tara Kugelman^a, Oluyemi O. Olumolade^a, Camilo Acosta^a, Tao Sun^a, Yang Han^a, Hermes A.S. Kamimura^a, Vernice Jackson-Lewis^{c,d,e,f}, Serge Przedborski^{c,d,e,f,*}, Elisa Konofagou^{a,b,*,2}

^a Departments of Biomedical Engineering, Columbia University, New York, NY 10032, USA

^b Departments of Radiology, Columbia University, New York, NY 10032, USA

^c Departments of Pathology & Cell Biology, Columbia University, New York, NY 10032, USA

^d Departments of Neurology, Columbia University, New York, NY 10032, USA

^e the Center for Motor Neuron Biology and Disease, Columbia University, New York, NY 10032, USA

^f the Columbia Translational Neuroscience Initiative, Columbia University, New York, NY 10032, USA

ARTICLE INFO

Keywords:

Focused ultrasound
Neurodegeneration
Blood-brain barrier
Neurotrophic factor
Neurorestoration

ABSTRACT

The blood-brain barrier (BBB) prevents most drugs from gaining access to the brain parenchyma, which is a recognized impediment to the treatment of neurodegenerative disorders like Parkinson's disease (PD). Focused ultrasound (FUS), in conjunction with systemically administered microbubbles, opens the BBB locally, reversibly and non-invasively. Herein, we show that neither FUS applied over both the striatum and the ventral midbrain, without neurotrophic factors, nor intravenous administration of neurotrophic factors (either through protein or gene delivery) without FUS, ameliorates the damage to the nigrostriatal dopaminergic pathway in the sub-acute MPTP mouse model of early-stage PD. Conversely, the combination of FUS and intravenous neurotrophic (protein or gene) delivery attenuates the damage to the nigrostriatal dopaminergic pathway, by allowing the entry of these agents into the brain parenchyma. Our findings provide evidence that the application of FUS at the early stages of PD facilitates critical neurotrophic delivery that can curb the rapid progression of neurodegeneration while improving the neuronal function, seemingly opening new therapeutic avenues for the early treatment of diseases of the central nervous system.

1. Introduction

The blood-brain barrier (BBB) poses a formidable impediment to the treatment of adult-onset neurodegenerative disorders, like Parkinson's disease (PD), preventing most drugs from gaining access to the brain parenchyma. Drug delivery techniques aimed at overcoming the almost impermeable BBB can be grouped into two main categories: (i) invasive and targeted and (ii) non-invasive and non-targeted methods. Direct injection, convection-enhanced delivery and osmotic BBB disruption are some examples of the first group while biological and chemical approaches as well as intranasal drug delivery belong to the latter group [1,2]. However, technological advances of the past decades have revealed the immense potential of therapeutic ultrasound in transcranial applications.

Focused Ultrasound (FUS) has been shown to produce a safe disruption of the BBB in various animal species and in experimental models of human diseases. The localized energy delivery coupled with the circulation of intravenously administered microbubbles initiates biological effects that are confined to the vessel walls only and contained solely within the targeted region [3]. Within a certain parametric range, the integrity of the BBB can be restored within hours and remain intact [4]. This technique has shown efficacy in delivering various compounds like contrast agents [5], sugars [6], antibodies [7], chemotherapeutics [8] and neurotrophic factors [6] into the brain parenchyma. Recent findings elaborate on the advantages of FUS-mediated gene delivery over conventional techniques [9–11] while initial clinical feasibility, safety and efficacy have been reported in the treatment of glioblastoma in > 15 patients [12].

* Corresponding authors at: Department of Radiology and Department of Neurology, Columbia University, New York, NY 10032, USA.

E-mail addresses: sp30@columbia.edu (S. Przedborski), ek2191@columbia.edu (E. Konofagou).

¹ These authors have contributed equally.

² These authors are co-senior authors.

The adherence of this study on trophic factors in PD stems from the large body of literature showing that neurotrophic factors such as glial-derived neurotrophic factor (GDNF) and neurturin (NTN) can impede the degeneration of the dopaminergic (DA) neurons in the substantia nigra pars compacta (SNc), and to restore the function of the injured DA neurons in experimental models of PD [13–15]. Furthermore, both GDNF and NTN have been tested in humans. Intraputamenal infusion of GDNF [16,17] resulted in functional improvement in 15 advanced PD patients as reported by two Phase I clinical trials, while the 25% amelioration in motor scores was not achieved in 17 out of the 34 PD patients in a phase II clinical trial. Likewise, intrastriatal delivery of the Adeno-associated type 2 viral vector encoding human NTN (AAV2-NTN) showed preventive effects on MPTP-induced motor disability in non-human primates, but clinical trials failed to show significant disease-modifying effects [18]. Despite the negative results of these Phase II studies, which might be due to technical issues [19–21], both GDNF and NTN remain quite appealing molecules for the present work given their well-established effects on the DA pathways [22,23].

Germane to this study, we have previously reported that FUS enhances the delivery of NTN in wild-type mice, non-invasively and locally at the level of PD-relevant brain regions [24]. Briefly, the area of NTN bioavailability, under the same ultrasound parameters as herein, was $5.07 \pm 0.64 \text{ mm}^2$ in the striatum (designated thereafter caudate-putamen [CPu]) and $2.25 \pm 1.14 \text{ mm}^2$ in the midbrain, showing the presence of NTN across the entire ultrasound-treated brain region compared to the relatively smaller region reached by direct injection. In this previous work, we also demonstrate that NTN cannot only be delivered successfully to the ventral midbrain through the FUS-induced reversible BBB-opening [24], but also that the permeate NTN retains its bioactivity as evidenced by the local activation of the downstream signaling pathway. This finding is particularly significant since the nigrostriatal pathway, which connects the SNc with the CPu, is the most severely-affected DA pathway in PD [25].

Relevant to our work is the demonstration by Fan et al. [10] of the restoration of the DA nigrostriatal pathway and reversal of motor deficits in a rat model of late-stage PD by combining FUS and non-viral vector-based gene therapy. This was the first report that addressed BBB opening and drug delivery in a PD model. Specifically, the authors used a neurotoxin-induced model of PD, which is characterized by a near complete acute destruction of the ipsilateral nigrostriatal pathway, hence emulating late-stage PD [26,27]. One of the salient results of this study is the demonstration of motor improvements in 6-OHDA-lesioned rats following FUS-assisted transfection for GDNF.

While the study of Fan et al. [10] provides major impetus to the use of ultrasound technology for therapeutic purposes, it also raises an important question. In advanced stages of PD, non-motor symptoms become a significant part of the disease as do cognitive decline and psychiatric and autonomic dysfunction, which can often become more troublesome than the cardinal motor manifestations of PD [28]. These disabling non-motor manifestations have been attributed to the degeneration of non-DA pathways, which arise over the course of the disease [28,29] and which are typically not responsive to either DA therapies (e.g. L-DOPA administration) or deep brain stimulation. Conversely, in early stage PD, patients are highly responsive to DA stimulation [29] hence, raising the question as to whether the targeting of the nigrostriatal pathway by the combined use of ultrasound and neurotrophic factors may not be of much greater clinical significance if applied sooner rather than many years after the emergence of PD manifestations. This is a particularly important question as patients with early PD are physically and professionally active [29] and most are reticent to use L-DOPA because of its known side effects. Thus, this study has been specifically designed to address not only the usefulness of FUS in allowing the delivery of BBB-impermeant bioactive molecules, but also whether such combined strategy might be more efficacious in improving the quality of life in patients afflicted by a neurodegenerative disorder, if applied early.

2. Materials and methods

2.1. Study design and animals

All experimental procedures involving animals were approved by the Columbia University Institutional Animal Care and Use Committee. Wild-type C57BL/6 mice (~25 g, ~3 months of age, sex: male, Harlan, Indianapolis, IN, USA) were group-housed under standard conditions (12 h light/dark cycles, 22 °C) and were provided with a standard rodent chow (3 kcal/g; Harlan Laboratories, Indianapolis, IN, USA) and water ad libitum. A total of 70 animals received a daily injection of MPTP (30 mg/kg free-base) for five consecutive days; this regimen causes an apoptotic degeneration of the nigrostriatal pathway in adult mice [30] and by ~21 d after MPTP administration, no further loss of nigral DA neurons is detected. The groups and the corresponding timeline are summarized in the Supplementary Fig. 1.

2.2. Focused ultrasound

Similar to our previous study, a single-element, spherical-segment FUS transducer (center frequency: 1.5 MHz, focal depth: 60 mm, radius: 30 mm; axial full-width half-maximum intensity: 7.5 mm, lateral full-width half-maximum intensity: 1 mm, Imasonic, France), driven by a function generator (Agilent, Palo Alto, CA, USA) through a 50-dB power amplifier (E&I, Rochester, NY, USA) was used to target the SN and the CPu. A central void of the therapeutic transducer held a pulse-echo ultrasound transducer (center frequency: 10 MHz, focal depth: 60 mm, radius 11.2 mm; Olympus NDT, Waltham, MA) used for alignment, with their two foci aligned. The imaging transducer was driven by a pulser-receiver (Olympus, Waltham, MA, USA) connected to a digitizer (Gage Applied Technologies, Inc., Lachine, QC, Canada). A bolus of 0.1 $\mu\text{L/g}$ of body mass polydisperse manufactured in-house [31] microbubbles diluted in saline ($8 \times 10^8 \#/\text{ml}$, mean diameter: 1.4 μm) was injected intravenously immediately preceding the sonication of each target, i.e. SN or CP. A 20-min time interval was allowed between SN and CPu (add Mania) targeting to allow the microbubble concentration to be cleared from the circulation [32]. Each animal was sonicated for 60 s, with a pulse repetition frequency (PRF) of 10 Hz, with one sonication location at SN and two sonication locations at the CPu in order to safely open the entire area of interest with acoustic parameters that do not cause damage, at peak negative acoustic pressure (PNP) of 0.45 MPa [33,34] after accounting for 18% and 33% murine skull attenuation for the SN and CPu, respectively.

2.3. Microbubbles

Polydisperse microbubbles were manufactured in-house following our previously published protocol [34]. Briefly, the 1,2-distearoyl-sn-glycero-3-phosphocholine (DSPC) and polyethylene Glycol 2000 (PEG2000) were mixed at a 9:1 ratio. Two milligrams of the mixture were dissolved in a 2 ml solution consisting of filtered PBS/glycerol (10% volume)/propylene glycol (10% volume) using a sonicator (Model 1510, Branson Ultrasonics, Danbury, CT, USA) and stored in a 5 ml vial at 4 °C. The empty space in the vial was filled with decafluorobutane (C_4F_{10}) gas and activated via mechanical agitation using a VialMix™ (Lantheus Medical Imaging, N. Billerica, MA) shaker for a pre-set time of 45 s. The concentration and size distribution of each microbubble vial were measured with a Coulter Counter Multisizer (Beckman Coulter Inc., Fullerton, CA).

2.4. Magnetic resonance imaging (MRI)

MRI was performed on mice receiving sonications. Upon completion of the ultrasound procedures, the BBB opening was confirmed with a 9.4 T MRI system (Bruker Medical, Boston, MA). The mice were placed in a birdcage coil (diameter 3 cm), while being anesthetized with 1–2%

isoflurane and vital signs monitored throughout the imaging sessions. A bolus of 0.3 ml of gadodiamide (GD-DTPA) (Omniscan®, GE Healthcare, Princeton, NJ) was injected intraperitoneally into each mouse. Approximately 50 min post the injection, MR images were collected using a contrast-enhanced T1-weighted 2D FLASH sequence [5]. In addition, T2-weighted MRI was performed 24 h post sonication to inspect the potential occurrence of edemas. Three-dimensional images were reconstructed using T1 images to visualize the BBB opening (Amira, FEI, Hillsboro, OR).

2.5. Simulation

The acoustic properties of the mouse head were obtained from microCT images with a resolution of 80 μm in the three directions (R_mCT2, Rigaku, Tokyo, Japan). The acoustic properties of the skull and the brain were obtained from previously published experimental data [35]. The numerical simulations were performed using the k-Wave MATLAB (MathWorks Inc., Natick, MA, USA) toolbox [36]. The toolbox provides the k-space pseudo spectral time domain solution for the coupled first-order acoustic equations for heterogeneous media. The detailed explanation of simulation parameters can be found in our previous report [37].

2.6. Neurotrophic factors

Recombinant human Neurturin was purchased from Invitrogen (CA, USA) and reconstituted according to the manufacturer's instructions. An intravenous injection of 50 μl Neurturin (20 $\mu\text{g/g}$ of body mass) followed immediately after the FUS-induced BBB opening for which 5 μl /mouse microbubbles were diluted in 100 μl saline and injected via the tail vein.

The AAV1-CAG-eGFP-GDNF vectors used in this study were purchased from SignaGen Laboratories (Rockville, MD). The titers of the viral vectors were provided by the manufacturer (quantified with real-time PCR) and diluted to 1.2×10^{12} GC/ml in PBS. For each mouse (average body weight of 25 g), a total of 100 μl diluted AAV was mixed with approximately 5 μl /mouse microbubbles and co-injected via the tail vein.

2.7. AAV transduction

The mice were sacrificed and the brains processed similar to the previous description but, the sections were treated with rabbit anti-GFP antibody (dilution 1:5000, Novus Biologicals, Littleton, CO) and goat anti-rabbit conjugated with Alexa Fluor 488 (dilution 1:500, ThermoFisher, Waltham, MA) to confirm AAV transduction. Fluorescence images were taken with a confocal microscope (Nikon Instruments Inc., Melville, NY).

2.8. Immunohistochemistry

Mice were subjected to transcardial perfusion upon sacrifice and the brains extracted, frozen and sectioned with a cryostat (30 μm) throughout the entire CPU and SN as previously described [24]. Every 6th section of the posterior CPU and SN, and every 6th section of the anterior CPU were processed free-floating for tyrosine hydroxylase (TH)-immunohistochemistry. Then, sections were sequentially washed in 0.1 M Tris-buffered Saline (TBS; pH 7.4), treated with 10% methanol/3% H₂O₂ solution in TBS, rewashed in TBS, incubated for 60 min in 5% normal goat serum (NGS, Vector, USA), and incubated for 49 h with an anti-TH antibody (Calbiochem, USA, 1:2000 for SN; 1:1000 for CPU) at 4 °C in TBS containing 2% NGS. Then, sections were washed in TBS, followed by incubation for 60 min with a secondary biotin-conjugated anti-rabbit antibody raised in goat (1:400 in TBS), washed again in TBS, incubated for 60 min in an avidin-biotin complex solution (ABC HRP kit (Peroxidase, Goat IgG), Vector Laboratories,

USA) in TBS, and then washed in TBS. Finally, immunostaining was visualized by 3,3'-diaminobenzidine (DAB substrate kit, Vector Labs) and all sections were counter-stained with cresyl violet solution (1 g cresyl violet acetate, Sigma-Aldrich, USA, in 500 ml DI-water with 25 ml acetic acid 10%).

2.9. Real-time PCR

Real-time PCR was used to quantify copies of GFP mRNA in various brain regions. Ten days after FUS-facilitated AAV delivery, mice were sacrificed and brain structures (striatum and substantia nigra) were isolated. The primers used in this study were forward (5'-AGCTGAAGGGCATCGACTTC-3') and reverse (5'-CTACGGCTACCTTGTTACGA-3'). The analysis was performed with a RNeasy Plus Mini Kit (Qiagen, Hilden, Germany). The mRNA levels were measured by qPCR using the SYBR Green assay (Applied Biosystems, Carlsbad, CA, USA). Signals from structures of interest were compared to signals from background tissue (cerebellum) and fold changes were obtained.

2.10. High-performance liquid chromatography (HPLC)

HPLC with electrochemical detection was employed to quantify the levels of dopamine, DOPAC and HVA. Following the same timeline for single NTN administration, mice (3–5 per group) were decapitated, their brains were quickly removed, hemispheres were separated and the corresponding sections (striatum and midbrain) were dissected out freehand on an ice-chilled glass petri dish. Samples were immediately frozen on dry ice and stored at -80 °C until analysis. On the day of the assay, the samples were sonicated in 50 vol (wt/vol) of HeGA while on ice. Centrifugation at 10,000 \times g at 4 °C for 10 min was followed by filtering and injection of the supernatant (20 μl) onto a C18-reverse-phase HR-80 catecholamine column (ESA, Bedford, MA). The samples passed through a mobile phase of 90% 50 mM sodium phosphate/0.2 mM EDTA/1.2 mM heptanesulfonic acid (pH = 3.5) solution and 10% methanol with a 1.0 ml/min flow rate. Peaks were detected by an ESA model Coulochem 5100A detector (E1 = -0.04 V, E2 = $+0.35$ V).

2.11. Quantitative morphology

The total number of TH- and cresyl violet-stained SNc neurons were counted by Stereology using the optical fractionator as per the published protocols as described in the Materials and Methods' section [38,39]. To quantify the immunoreactivity of TH+ nerve fibers in the SN pars reticulata (SNr), midbrain tissue sections were white-balanced, and color deconvoluted [24,40] prior to being converted to grayscale. Then, the SNr was manually outlined, and the pixels within this region of interest (ROI) were thresholded. The percentage of the dendrites/axons-covered area on each side, i.e. ipsilateral and contralateral to FUS, was determined and the average ratio of each group was used to compare the results among the different groups. The same quantification algorithm, presented in Supplementary Fig. 2, was followed for the TH+ expression in the CPU images without the deconvolution step since the striatum slices were not counterstained.

2.12. Stereology

Estimates of the number of TH+ neurons in the SNc were generated by first delineating the borders of the SNc with a $5\times$ objective using the anatomical landmarks specified in the literature [41,42]. The number of SNc TH+ (DA) neurons was then calculated using the optical fractionator probe (Stereoinvestigator, version 11.02.1, MBF Bioscience, Williston, VT, USA) and with the sampling parameters empirically determined by Baquet et al. [42] or the mouse SN. By applying a random start and random distribution of the counting frames, every 6th section was counted (for a total of ~ 10 sections per mouse) with an unbiased counting frame size of 100×100 μm and a grid size of 200×200 μm .

Cells were sampled through the entire thickness of the tissue section using a 1 μm guard zone. Sections were viewed under a 40 \times dry objective. At least 100 cells were counted within 40–60 framing sites for each side and animal, and the coefficient of error was ≤ 0.10 .

2.13. Behavioral Study

Amphetamine-elicited behavioral outcomes attributed to neurorestorative effects were investigated. Four weeks after MPTP lesioning, mice were randomly assigned to four groups. Each mouse received an intraperitoneal injection of amphetamine (2.5 mg/kg, dissolved in 150 μl saline) 10 min before behavioral testing. The subject was then placed in an open field chamber consisting of a custom-made polycarbonate chamber (dimensions: 27.3 cm \times 27.3 cm \times 27.3 cm). Directly above the chamber was a video camera, which interfaced with a computer and tracking software (Noldus, Wageningen, Netherlands). Each subject was placed directly in the center of the field, and video tracking was used to record and measure activity. Mice explored the field ad libitum for a session duration of 40 min. Upon completion, the subject was removed, urine and feces were counted and removed, and the chamber was cleaned with ethyl alcohol and disinfectants to remove any trace of the former subject. The same behavior testing was repeated for each animal post AAV/FUS treatment at the end of the 12-week survival period.

2.14. Statistical Analysis

Intra-group comparisons between the ipsilateral and contralateral sides were analyzed using a two-tailed paired Student's *t*-test. All values are expressed as means \pm standard deviation. Differences among group means were analyzed using two-way factorial analysis of variance (ANOVA) with AAV and FUS as the independent factors. When ANOVA showed significant differences, pair-wise comparisons between means, post-hoc analysis by Newman-Keuls multiple comparisons test was performed. In all analyses, the null hypothesis was rejected at the 0.05 level. All statistical analyses were performed using Prism 7 (Graphpad Software, San Diego, CA, USA).

3. Results and discussion

To determine the potential value of using FUS to improve brain penetrance of bioactive molecules, especially those promoting functionality, if not viability, of the compromised neurons in certain regions of the neurodegenerated brain, we elected to use the MPTP mouse model of PD [25]. More precisely, not only does this neurotoxin-based model provide, in mice, reliable, extensively-validated lesioning of specifically the nigrostriatal DA pathway, but also causes, in humans, a clinical picture almost indistinguishable from PD [43], hence strengthening the relevance of the anticipated mouse findings to the human condition. It should also be emphasized that most effective preclinical neuroprotective strategies tested in animal models of PD, while mitigating neurodegeneration, fail to maintain DA function [44], hence often ending with a number of SNc neurons unable to produce DA. Thus, the importance of identifying adjunct strategies that are capable of improving function in spared DA neurons is critical to the success of neuroprotective/neurorestorative strategies. Accordingly, our preclinical experiments were designed to be specifically relevant to this important clinical issue by using, primarily, TH-immunostaining and quantitative morphology in the nigrostriatal DA pathway of mice post-MPTP as a proxy for FUS allowing NTN and GDNF to reach and to operate within the CNS. This strategy was prompted by the fact that many spared DA neurons in the MPTP model have subnormal expression of TH, the rate-limiting enzyme in DA synthesis, and that neurotrophic factors have the property of stimulating TH expression.

For the present study, the workflow focused on the morphological

quantification of cell bodies, dendrites and nerve terminals of the nigrostriatal DA pathway (see Materials and Methods' section and Supplementary Fig. 2). Our experimental design compared TH-based parameters between hemispheres among MPTP-injected mice that received either no, one or three systemic injections of NTN combined with either one or three unilateral brain FUS exposures or a single gene delivery of AAV-GDNF; throughout this study, the ipsilateral hemisphere refers to the hemisphere receiving the unilateral ultrasound. Previously, we used a similar design in intact mice and found that the application of unilateral brain FUS following a systemic injection of another trophic factor, BDNF, did promote its entry into the brain, only in the ipsilateral hemisphere and in a highly regionally restricted manner [6]. In a similar rationale, the successful delivery of NTN through the FUS-induced BBB opening in wild type mice has been confirmed by tracing the downstream signaling pathway through the detection of increased phosphorylation of the Ret receptor, cytoplasmic kinase Erk 1 and 2 and CREB transcription factor in structures associated with their abundance [24]. Also, for the purpose of this study, the neurotrophic factors are assumed to be of equivalent efficacy when it comes to neurorestoration and neuroprotection as previously reported [45,46].

3.1. MPTP suppresses TH immunoreactivity in the CPu and midbrain under a sub-acute regime

As we have previously demonstrated [47], the regimen of MPTP used here in adult mice not only causes a loss of TH-positive cell bodies in the SNc, but also, and to a greater extent, of TH-positive dendrites in the SNr and nerve terminals in the CPu. As shown in Fig. 1, mice that were subjected to this subacute regimen of MPTP conformed to the known description of the aforementioned brain lesion. However, based on our past experience [47], we specifically set the dosage of MPTP per injection to cause a detectable but minimal reduction in TH-positive neurons in the SNc so that we could predict a 40–50% reduction in TH-immunoreactivity in the CPu. This approach was selected since the goal for this work was to closely emulate an early stage of PD [25]. Indeed, the ultimate objective of the proposed methodology would be for application in early stage PD patients who may experience a particularly strong quality of life improvement, should the proposed therapeutic strategy effectively boost the expression of DA synthetic enzymes, such as TH, in compromised, but still alive SNc neurons. As expected, our stereology counts revealed a $\sim 23\%$ reduction of SNc TH-positive neurons in mice injected with MPTP compared to those injected with saline (two-way ANOVA for $n = 7$, $F[1, 12] = 3.191$; $P = 0.0993$). To assess the effect of MPTP in the SNr and CPu, we used a customized TH density quantification algorithm based on thresholding (see Materials and Methods' section and Supplementary Fig. 2). Images were white-corrected and color-deconvoluted before delineating the SNr or the CPu as the ROIs. The percentages of pixels over the ROIs that exceeded the set intensity threshold for both MPTP- and saline-injected mice are presented for both hemispheres separately (Fig. 1). Based on this method, we found that MPTP-injected mice displayed a $\sim 35\%$ and $\sim 45\%$ reduction of TH-immunoreactivity in the SNr (two-way ANOVA for $n = 5$, $F[1, 8] = 5.335$; $P = 0.0497$) and CPu (two-way ANOVA for $n = 5$, $F[1, 8] = 25.64$; $P = 0.0010$), respectively. Furthermore, neither in the MPTP-treated (pair Student's *t*-test; SNc: $t[6] = 0.821$, $p = 0.442$; SNr: $t[4] = 0.07$, $p = 0.947$; CPu: $t[4] = 1.832$, $p = 0.14$) nor in the saline-administered mice (pair Student's *t*-test; SNc: $t[6] = 0.217$, $p = 0.835$; SNr: $t[4] = 1.447$, $p = 0.221$; CPu: $t[4] = 0.426$, $p = 0.691$) did the DA parameters differ significantly between the two hemispheres, excluding TH-immunoreactivity asymmetry. The significant loss of cell bodies, dendrites and terminals in the MPTP brains was also noted by the decreased TH immunoreactivity shown in Fig. 1b–d compared to the saline group.

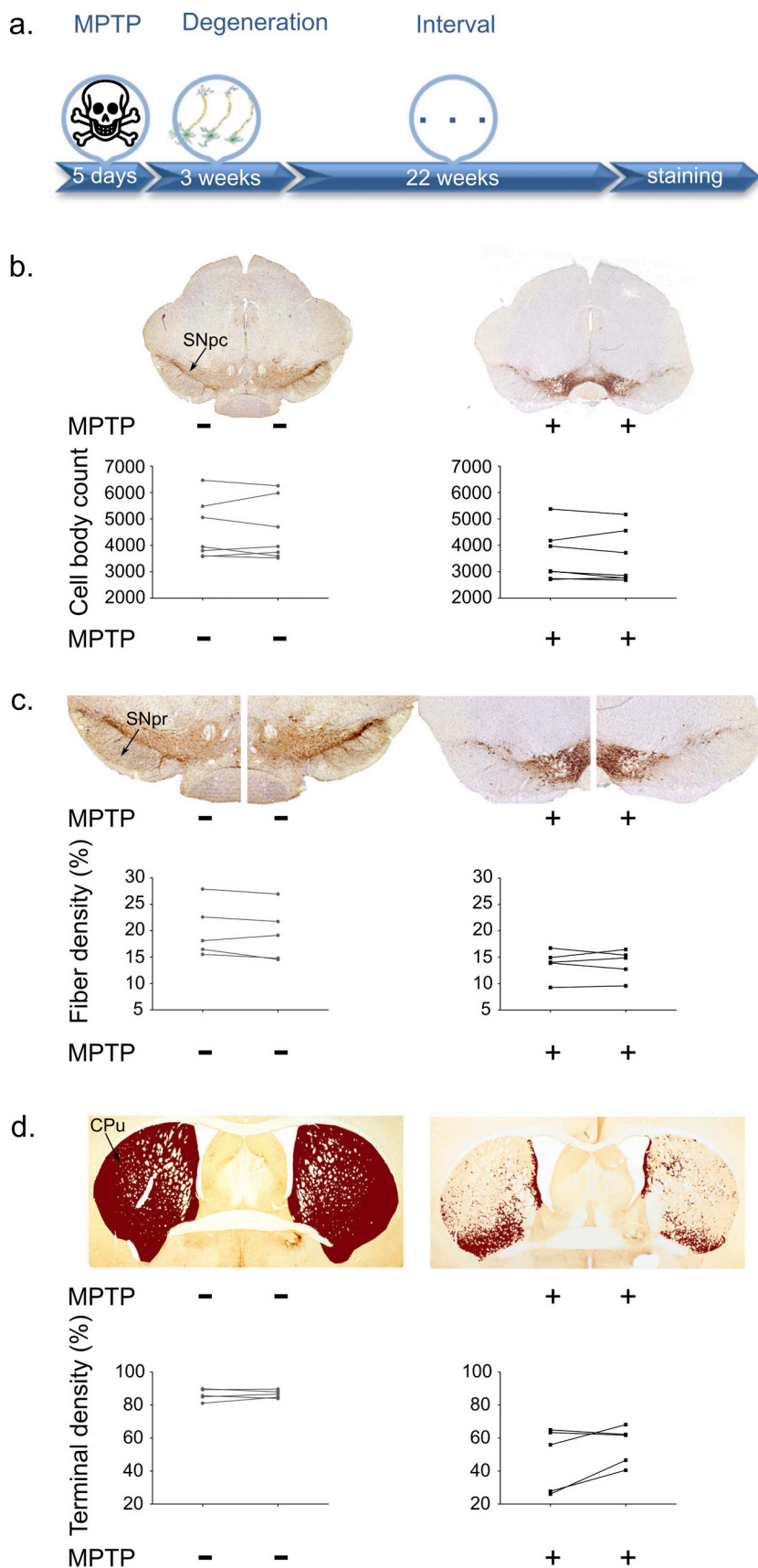


Fig. 1. The MPTP effect. a. The timeline shows degeneration following MPTP application and the interval until immunohistochemistry was performed. b. Representative coronal images of the SNc for control and MPTP injected groups. SNc cell body quantification for each brain hemisphere is presented. A ~22% reduction of SNc TH+ cell body number is observed in the MPTP- vs saline-injected mice (two-way ANOVA for $n = 7$, $F_{[1, 12]} = 3.191$; $P = 0.0993$). c. Higher magnification (4x) images focusing on the SNr shows a loss of fibers of ~33% in MPTP- vs saline-injected mice (two-way ANOVA for $n = 5$, $F_{[1, 8]} = 5.335$; $P = 0.0497$). The area quantification is presented per hemisphere and per brain. d. Representative images of the CPu TH+ terminal density for the saline and MPTP groups showing a ~40% reduction of CPu TH+ immunoreactivity in MPTP- vs saline-injected mice (two-way ANOVA for $n = 5$, $F_{[1, 8]} = 25.64$; $P = 0.0010$). Area quantification shows the decrease in TH+ immunoreactivity for the MPTP mice per side per brain.

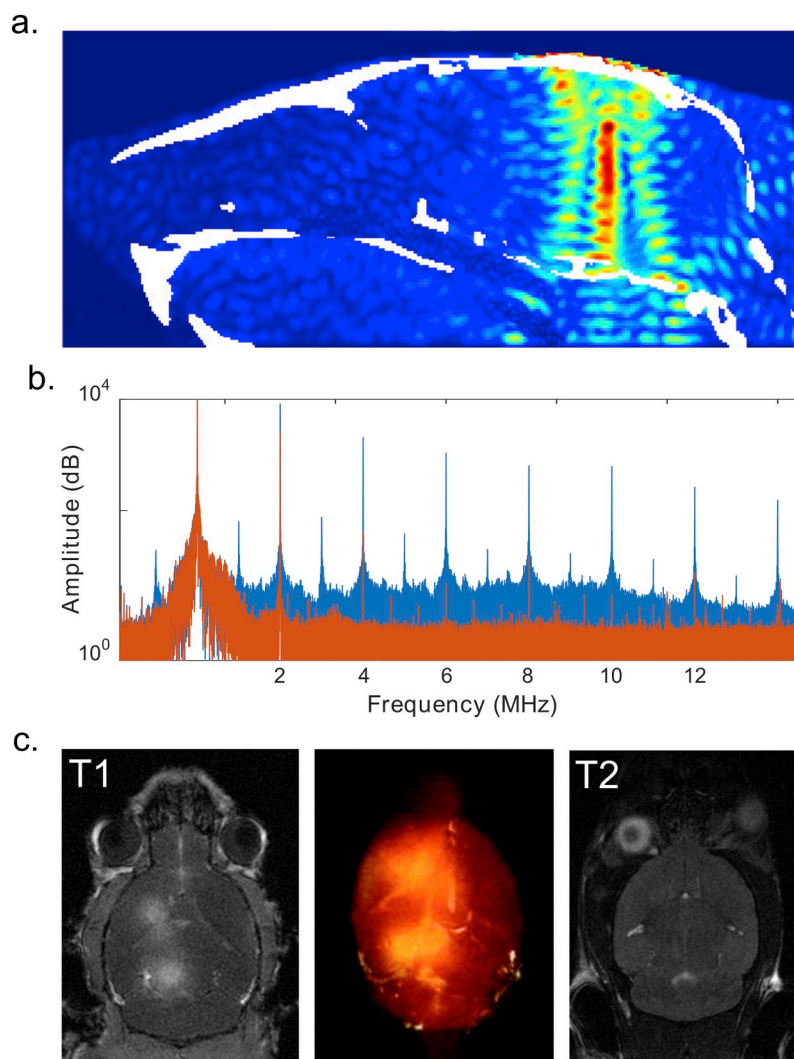


Fig. 2. FUS-facilitated delivery. a. CT-based simulation revealed the FUS beam focus in situ (mouse skull is indicated in white). b. Passive cavitation detection was used to monitor the sonication in real-time without (orange) and with (blue) microbubbles. c. BBB opening was confirmed with contrast-enhanced T1-weighted MRI (left) and rendered in 3D (middle). No edema was observed on T2 MRI one-day post sonication.

3.2. FUS-facilitated BBB opening

The BBB is virtually impermeable to macromolecules (including NTN and AAV) due to the contributions of tight junctions, pericytes, and astrocyte end feet [48]. In order for the macromolecules to reach the targeted brain parenchymal region, the local BBB has to be temporarily opened. The acoustic energy, amplified by microbubbles, exerts mechanical forces on the endothelial cells as well as on surrounding BBB components [49]. Simulations were performed to optimize the sonication parameters using mouse computed tomography (CT) scans. As illustrated in Fig. 2a, the focused acoustic beam concentrated in the targeted region (indicated in red) and the -3 dB acoustic pressure field was estimated to be $1 \times 1 \times 7.5 \text{ mm}^3$. The effectiveness of the delivered ultrasound energy was monitored in real-time using a passive cavitation monitoring system, which captured the signals emitted from the cavitating microbubbles [50]. As shown in Fig. 2b, the orange signal indicated the pre-microbubble administration baseline signal, while the blue signal demonstrates augmented ultrasound-microbubble interaction in situ. The successful disruption of the BBB was evaluated via contrast-enhanced T1-weighted MRI as shown in Fig. 2c. The BBB-opened regions are highlighted via diffused MR contrast agent gadolinium. A three-dimensional rendering of the opening is also illustrated in Fig. 2c. In addition, T2 scans were performed to identify the presence

of potential edema caused by the sonications. Under the ultrasound parameters used in this study (frequency of 1.5 MHz and peak negative pressure of 0.45 MPa), we did not observe short-term (one-day post sonication) edema, as evidenced in the T2-weighted MRI.

3.3. Protein delivery upregulates the depleted DA neurons in the SN region

Having established the damage caused in the three selected brain regions, i.e. SNc, SNr, and CPU by the MPTP injections (Supplementary Fig. 3), we then investigated the effects of the combination of a unilateral brain FUS application with the systemic administration of NTN on DA parameters in MPTP mice. Given the lack of right-left DA asymmetry in the MPTP mice reported above and the fact that FUS is applied only on one side of the brain, our results were computed as ratios of ipsilateral over contralateral values to better capture the unilateral nature of the proposed strategies.

Since the cell bodies of the nigrostriatal DA neurons reside in the SNc, assessment of the effect of FUS/NTN in this specific brain region was first performed in order to understand the potential effect of our methodology on a stable lesion, i.e. fixed number of neurons. Indeed, at the selected time point, it has been demonstrated previously that DA neurons no longer die [51]. Since no compelling evidence of DA neurogenesis in the post-lesioned adult brain exists [52], any change in the

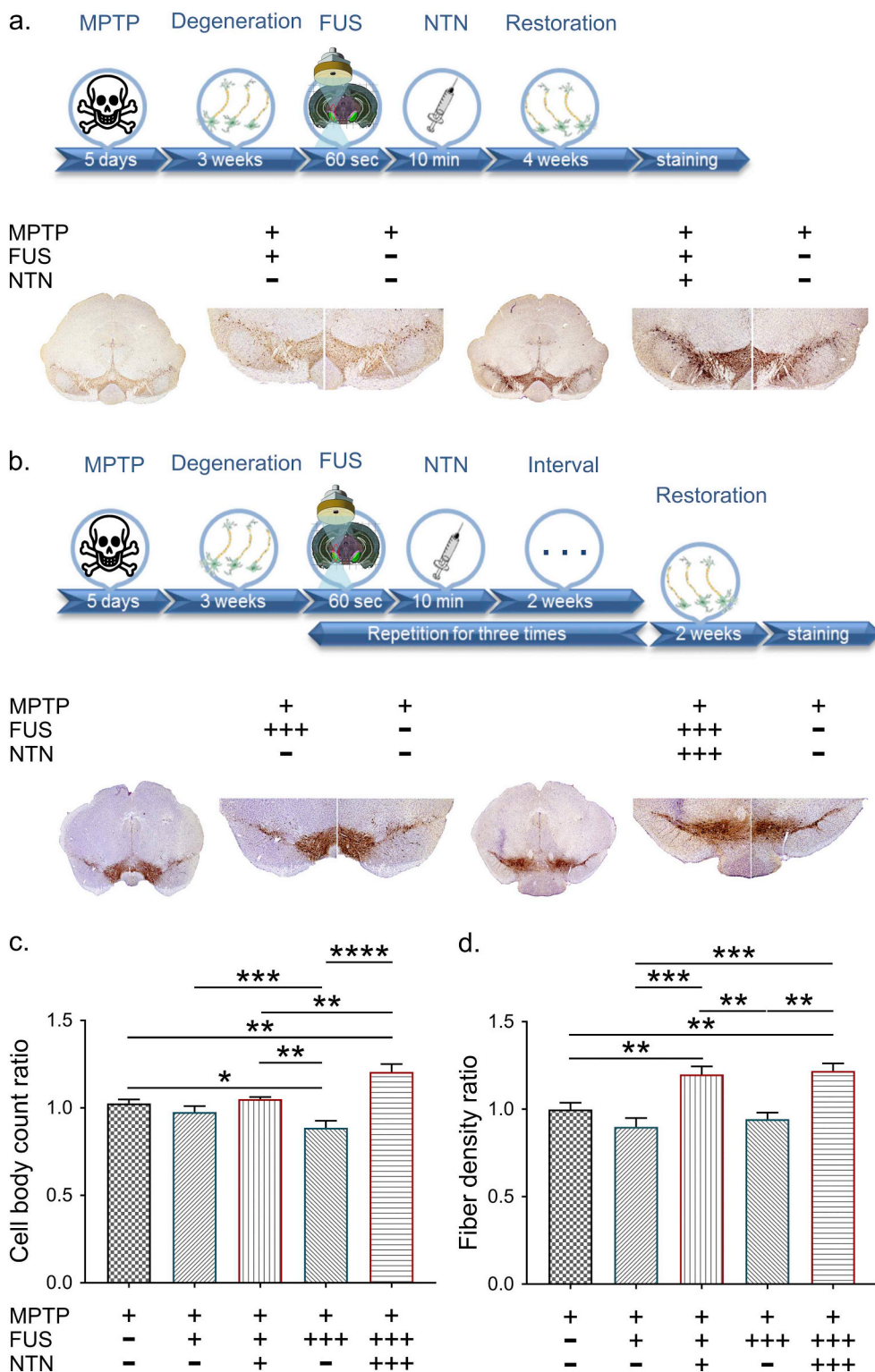


Fig. 3. Neurorestoration effect at the level of the SN. a. Single treatment at the SN: The descriptive timeline of the procedure is followed by representative TH immunohistochemistry images. The plus/minus signs indicate whether the corresponding side of the brain received MPTP, FUS and NTN. b. Triple treatment at the level of the SN: The corresponding timeline provides information regarding the additional steps followed for this part of the study. The plus/minus signs indicate whether the brains received MPTP, FUS and NTN and the three plus signs denote the times the treatment was repeated. c. Cell body counts at the level of the SNc region. Results are shown as the relative ratio by dividing the contralateral side into the ipsilateral side. The statistical significance occurs with one-way ANOVA ($n = 5-7$; $F_{[4, 27]} = 8.892$; $P = 0.0001$) after correcting the multiple measurements with Newman-Keuls method. d. The area quantification of the fibrotic density at the SNr region. The results are shown as the relative ratio by dividing the contralateral side into the ipsilateral side. The statistical significance occurs with one-way ANOVA ($n = 5-7$; $F_{[4, 22]} = 11.31$; $P < 0.0001$) after correcting the multiple measurements with Newman-Keuls method.

number of TH-positive neurons could only be attributed to a larger number of “countable neurons” due to increased TH immunoreactivity. This phenomenon, thus, works as a proxy for NTN action. Two descriptive timelines show the steps followed during the experimental procedure for the single and triple treatment separately, along with the representative TH-immunostained tissue sections (Fig. 3, Supplementary Fig. 4). A one-way ANOVA for the five groups of MPTP-injected mice, i.e. FUS-/NTN-, FUS+/NTN-, FUS+++/NTN-, FUS+/NTN+, and FUS+++/NTN+++, revealed significant differences in SNc TH-

positive neuron numbers ($n = 5-7$; $F_{[4, 27]} = 8.892$; $P = 0.0001$). By using Newman-Keuls post-hoc tests, we found that either one or three FUS applications to MPTP mice alone failed to significantly increase TH-positive SNc neuron numbers compared to no FUS ($P > 0.05$). Conversely, administration of three, but not one, NTN administrations, each time preceded by FUS application, resulted in a significant increase ($p < 0.01$) on the order of 17%. Thus, these findings indicate that systemic NTN successfully gained access to the CNS following FUS application and initiated the upregulation of TH expression within the

spared SNc DA neurons. Although these results are encouraging, from a functional standpoint, it remains to be investigated whether similar changes occurred where DA neurotransmission actually takes place.

One unique property of SNc DA neurons is the capacity to release DA from their dendrites, suggesting that DA mediates neurotransmission events not only at the level of the CPU but also at the level of the SNr. Thus, to address the effect of NTN in the SNr region, the thresholded area covered by TH-positive fibers exceeding the stain-intensity cut-off was extracted and normalized to the entire region covered by fibers. As for the SNc, a one-way ANOVA revealed significant differences in SNr TH-positive fiber density among the five groups ($F_{[4, 22]} = 11.31$; $P < 0.0001$) as shown in Fig. 3d. As was the case with the cell bodies, the Newman-Keuls post-hoc test demonstrated that neither one nor three FUS applications alone to MPTP mice produced any positive changes in SNr fiber density. In contrast, both single and triple administration of NTN, after the corresponding applications of FUS, resulted in a statistically significant increase of the SNr TH-positive dendritic network on the order of 20–22% compared to the no FUS group. The higher TH-immunoreactivity observed within the SNr in response to FUS/NTN treatment supports the notion that dendritic expression of DA markers in spared neurons post-MPTP can be increased.

Furthermore, given that TH is the rate-limiting enzyme in DA synthesis, our results support the fact that the combination of NTN and FUS may help to enhance DA neurotransmission in compromised neurons. Interestingly, if enhanced DA neurotransmission within the SNr can be associated with comparable changes in the CPU, the proposed therapeutic strategy may have far-reaching implications for the symptomatic treatment of PD. It is also worth noting that since the magnitude of the changes was not significantly different in MPTP-injected mice that received one or three FUS/NTN treatments, it may be argued that, with respect to SNr, the maximal induction of TH in the DA dendrites is already achieved after a single FUS/NTN exposure. However, from the perspective of a chronic condition like PD, future studies will have to investigate the duration of the dendritic induction of TH produced by one and three FUS/NTN exposures and assess the recurrence of the treatment, as this question may be of major importance in determining the optimal FUS/NTN regimen for PD patients.

3.4. Repeated protein delivery is necessary to upregulate the DA terminals in the CPU

Anatomically, SNc DA neurons project primarily to the CPU [25], hence the loss of SNc DA neurons in PD causes a striatal depletion of DA nerve terminals and DA content. To determine the efficacy of our technique in promoting nerve terminal function, we estimated CPU fiber density by quantifying its TH immunoreactivity employing the same algorithm as for the SNr site. Fig. 4 shows the respective timelines with the sonicated structure as well as representative images for each group (Supplementary Fig. 5). Again, we performed a one-way ANOVA which revealed significant differences in the CPU TH-positive fiber density among the five groups ($n = 5-7$; $F_{[4, 24]} = 3.527$; $P = 0.0212$). As expected, from the preceding analysis of the SN regions, FUS alone did not result in an increase of the terminal TH positivity. In striking contrast to the situation observed in the SNr, only the three FUS/NTN exposures caused an overt increase in TH immunoreactivity in the CPU of the MPTP mice ($p < 0.05$) on the order of 50%. Since the single administration of NTN failed to permeate the CPU as effectively as in the SNr, the stronger regimen of FUS/NTN may be required to achieve the desired effect. Furthermore, within the CPU, TH-positive fibers represent < 10% of the fiber pool hence, most of the NTN molecules in the CPU might interact with neuronal structures other than TH-positive fibers. To complement these immunohistochemical findings, the levels of DA and its metabolites, homovanillic acid (HVA) and 3,4-dihydroxyphenylacetic acid (DOPAC) were determined by HPLC in both the ventral midbrain and striatum. The results are reported as ratios of ipsilateral over contralateral levels to capture the unilateral effect of

our intervention (Fig. 5). A significant twofold increase in DA levels was observed in the ventral midbrain ($F_{[3, 13]} = 7.055$; $P = 0.0047$) and to a lesser extent in the CPU of hemispheres treated once with ultrasound and NTN compared to the rest. The levels of the key metabolites followed the same trend, even though these changes in metabolites were not statistically significant. These HPLC findings are in agreement with the TH immunoreactivity proving the insufficiency of the single treatment in restoring the depleted DA to its original levels.

The decrease in TH immunoreactivity observed in MPTP-injected mice treated with ultrasound alone (FUS+/NTN- and FUS+++/NTN-) in Figs. 3 and 4 raised the possibility that FUS might downregulate TH expression. To test this possibility, naïve mice (i.e. not injected with MPTP) were subjected to FUS. For this experiment, five mice sonicated multiple times (MPTP-/FUS+++/NTN-) and five mice sonicated only once (MPTP-/FUS+/NTN-) were compared against five control mice (MPTP-/FUS-/NTN-); for the three sonications protocol, two days interval was used between each sonication to allow the BBB to be restored [4]. Remarkably, the number of SNc TH-positive neurons did not significantly differ among the three groups (one-way ANOVA, $F_{[2, 12]} = 1.755$; $P = 0.2145$). Similarly, no significant differences were observed in either the SNr TH-positive dendrite (one-way ANOVA, $F_{[2, 12]} = 0.1158$; $P = 0.8917$) or CPU TH-positive terminal density (one way ANOVA, $F_{[2, 12]} = 0.1193$; $P = 0.8886$) across the three groups (Supplementary Fig. 6). Although FUS does not cause any detectable alteration in TH expression in healthy neurons, it remains an open question whether ultrasound could downregulate TH expression in compromised neurons.

3.5. Gene delivery upregulates the depleted DA neurons in both the SN and CPU

To determine whether dopaminergic restorative effects could be produced by the combination of AAV-GDNF and FUS in the early stages of PD, a new cohort of mice was used and the different treatments (FUS-/AAV-, FUS+/AAV-, FUS-/AAV+, FUS+/AAV+) were compared 84 days after the delivery (Fig. 6a).

The viral vector used in this study was AAV1 under the control of the neuron-specific CAG promoter. Different from AAV9, a more aggressive serotype, AAV1 does not cross the BBB spontaneously, and yet maintaining a higher level of bioactivity compared to that of AAV2. Our previous work has shown that greater transduction can be achieved using this serotype compared to AAV2 [11], which has been the sole choice for all clinical PD trials to date [53]. The CAG promoter was selected to best represent the vector used in prior clinical trials. In this study, we observed some degree of non-specific transductions in untargeted organs, such as the liver and kidney similar to neuron-specific promoter synapsin [54,55].

Upon sacrifice, immunohistochemistry revealed stronger TH immunopositivity at the level of the ventral midbrain sections of MPTP mice receiving AAV+/FUS+ combinations, on the sonicated side, than at the level of ventral midbrain sections of mice from all other MPTP groups (Fig. 6b). Quantitatively, TH-positive neuron numbers did not significantly differ (paired Student *t*-test; $t_{[7]} \leq 0.45$, $p \geq 0.67$) in mice that received neither or one form of treatment (i.e. AAV or FUS) as shown in Fig. 6c (Supplementary Fig. 7). However, while marginal, MPTP mice that received systemic AAV-GDNF injection and unilateral sonication showed, on average, a greater number of SN TH-positive neuron numbers on the sonicated side (paired Student *t*-test; $t_{[11]} = 2.93$, $p = 0.015$). Even more striking is the observation that MPTP mice from the AAV+/FUS+ group showed, on the sonicated side, quite a stronger SN pars reticulata optical density of TH immunostaining (Fig. 6d and e) (paired Student *t*-test; $t_{[4]} = 7.01$, $p = 0.006$), suggesting that the combination of AAV-GDNF and FUS has a strong beneficial effect on dopaminergic dendrites. Across group comparison revealed a significant increase ($n = 4-5$; $F_{[3, 13]} = 7.514$; $P = 0.0036$) on the order of 76% in the dendritic fiber network of the

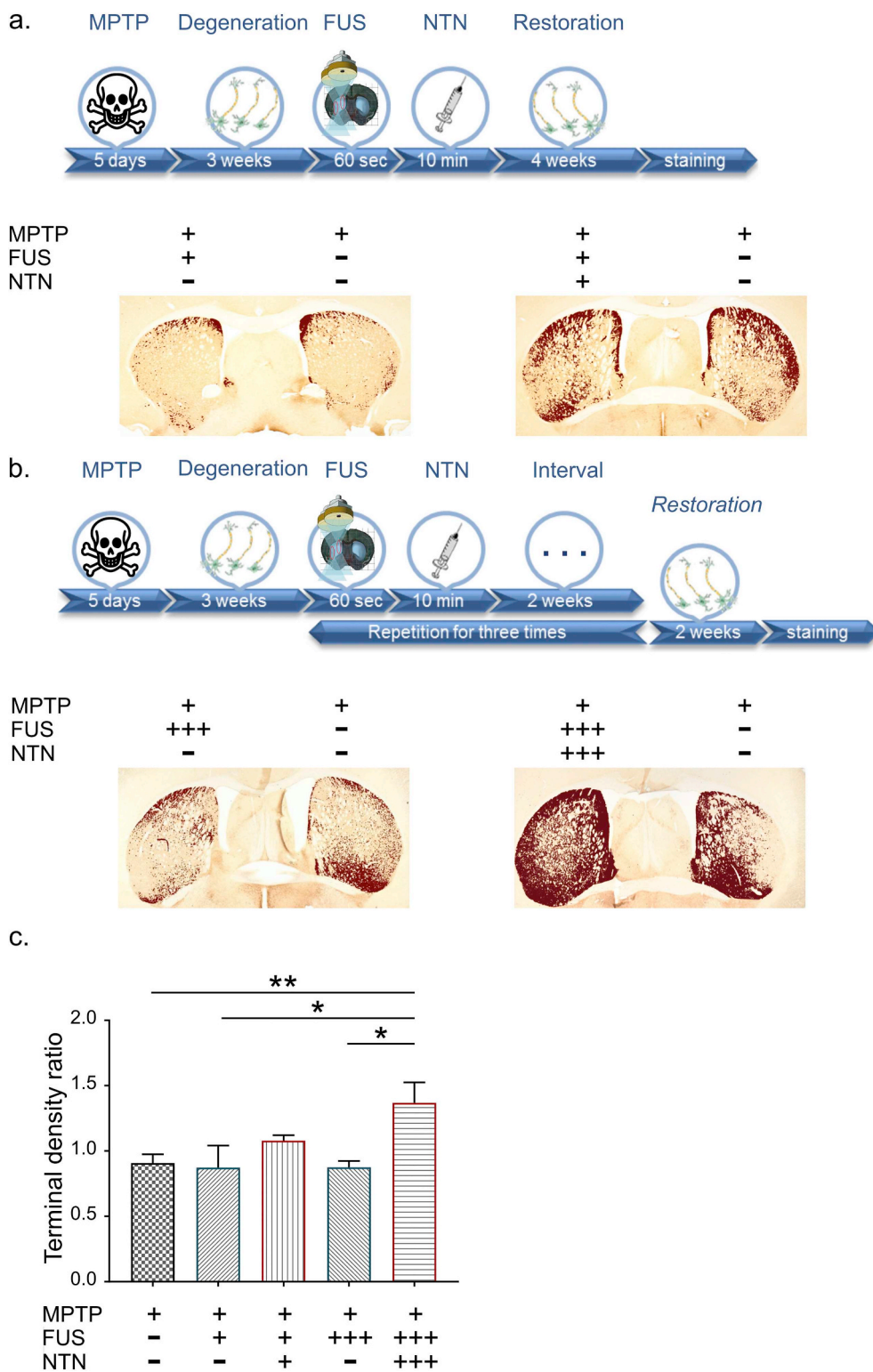


Fig. 4. Neurorestoration effect at the Caudate-Putamen (CPu) region. **a.** The descriptive timeline of the procedure is followed by representative TH immunohistochemistry images. The pixels surpassing a certain threshold are presented in dark red to enhance the differences between the ipsilateral and contralateral side. The plus/minus signs indicate whether the corresponding side of the brain received MPTP, FUS and NTN. **b.** Triple treatment at the CPu: The corresponding timeline provides information regarding the additional steps followed for this part of the study. The plus/minus signs indicate whether the brains received MPTP, FUS and NTN and the three plus signs denote the number of times the treatment was repeated. **c.** The area quantification of the terminal density at the CPu region. Results are shown as the relative ratio by dividing the contralateral side into the ipsilateral side. The statistical significance occurs with one-way ANOVA ($n = 5-7$; $F_{[4, 24]} = 3.527$; $P = 0.0212$) after correcting the multiple measurements with Newman-Keuls method permeate the CPu as effectively as in the SNr, it may be that the stronger regimen of FUS/NTN is required to achieve the desired effect. Furthermore, within the CPu, TH-positive fibers represent less than 10% of the fiber pool hence, most of the NTN molecules in the CPu might interact with neuronal structures other than TH-positive fibers.

ipsilateral-over-contralateral side compared to the MPTP group (Fig. 6e). A very similar situation was observed for the ratio of the striatal TH-positive terminal density which was significantly higher ($n = 4-5$; $F_{[3, 17]} = 4.733$; $P = 0.014$) on the order to 32% for the AAV +/FUS+ group compared to the MPTP-injected mice (Fig. 6f).

To provide a functional correlate to the above results, we took advantage of the fact that amphetamine, by stimulating the release of dopamine from the residual neurons, induces a rotational behavior in rodents if there is a right/left imbalance [56]. Using a camera-based

behavioral testing apparatus, mice were allowed to explore the field freely and the number of clockwise (CW; i.e. away from the sonicated hemisphere) and counter-clockwise rotations (CCW; toward the sonicated hemisphere) were recorded after amphetamine injection. After MPTP injection but prior to any AAV and/or FUS treatment, no significant rotational behavior was noted in any of the mice indicating that the MPTP lesion produced symmetrical damage (Supplementary Fig. 8). Twelve weeks after the AAV and/or FUS treatment, only the MPTP mice from the AAV +/FUS+ group showed significant rotations

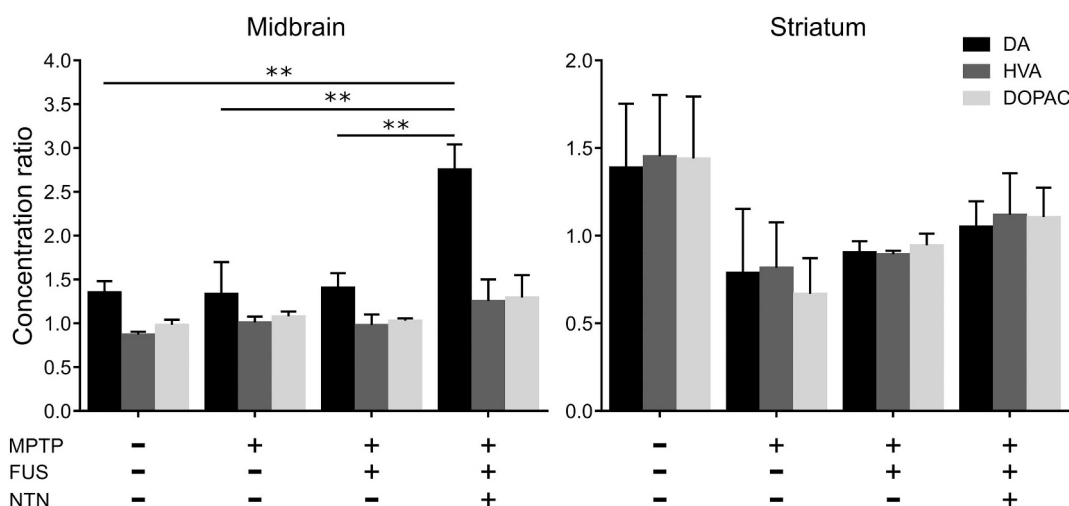


Fig. 5. HPLC analysis of dopamine (DA) and its key metabolites (HVA and DOPAC) in the ventral midbrain and the striatum. The results are reported as ratios of ipsilateral over contralateral levels to capture the unilateral effect of our intervention. A twofold increase in the levels of DA can be observed in the midbrain of the hemispheres treated once with ultrasound and NTN compared to the rest of the groups (one way ANOVA, $F_{[3, 13]} = 7.055$; $P = 0.0047$). This trend is preserved for the metabolites but lacks significance. This lateralized increased dopamine level was not observed in the striatum despite the small increase in the metabolites observed in the FUS/NTN group compared to the MPTP only group.

that were consistently CW (paired Student *t*-test; $t_{[8]} = 2.61$, $p = 0.035$), supporting the notion that the sonicated side was associated with higher amphetamine-induced dopaminergic neurostimulation (Fig. 6h).

The AAV+/FUS+/- treated mice had significantly higher optical densities for both the dendritic field in the SN pars reticulata and the nerve terminal network in the CPU, on the sonicated side as well as a marginal increase in SN TH-positive neurons on the sonicated side. Since no compelling evidence exists, supporting that novel dopaminergic neurons can be produced in mature brains [44], the most parsimonious explanation for the AAV/FUS-related changes in neuronal counts is that the combined treatment stimulates the expression of TH, causing merely more dopaminergic neurons to become identifiable and counted. Although this explanation can also apply to the dendritic field changes, we cannot exclude that the nerve terminal changes are, at least, due to axonal sprouting. While more work is required to elucidate the underpinning process driving the aforementioned changes, we already know that they are functionally relevant since, following amphetamine injection, the MPTP mice post-treated with AAV/FUS display a robust rotational behavior consistent with the idea that the sonicated side that received AAV-GDNF recovered a strong dopaminergic neurotransmission [56].

The therapeutic alternatives explored in this study showed a gradual increase in beneficial outcome. Direct protein delivery was proven efficient in upregulating neuronal function but its translation to the clinical practice entails multiple applications that significantly improve neuronal integrity along the entire pathway. Gene therapy comes as an alternative to multiple applications allowing for constant release of the neurotrophic factor with only one ultrasound session. The successful delivery was followed not only by upregulation of the dopaminergic pathway including a small increase in neuronal cells but also by a detectable behavioral effect enhanced by the administration of amphetamine.

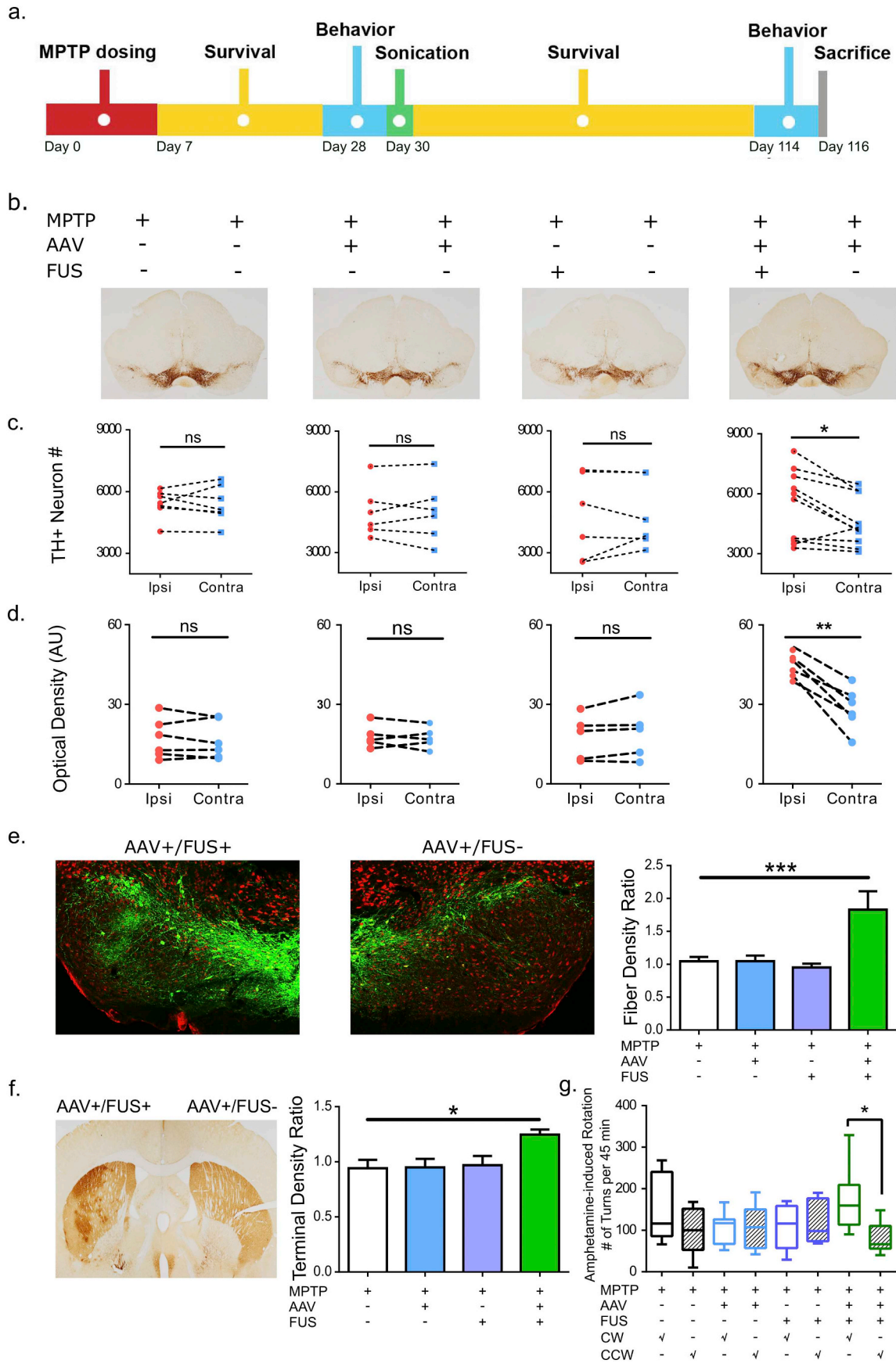
One limitation of this study is that FUS could induce acute inflammation in the sonicated region [57]. This is likely caused by the exudates (such as albumin) through the opened BBB leading to microglia upregulation. However, as shown in our previously reported studies, this does not lead to long-term inflammation nor behavior deficits [11]. The amount of administered viral vectors should also be carefully examined to minimize systemic toxicity and immune response. Studies in larger animal models (i.e. non-human primates) need to be carried

out before results presented here can be translated to the clinic.

Other limitations in this study include the limited number of mice used primarily due to the high cost of NTN acquisition. As a consequence, additional quantitative measures to directly measure DA synthesis such as analytical techniques could not be fully explored but will be included in future studies. Moreover, different dosages, upregulation duration as well as the time-interval between consecutive treatments also could not be studied. Multiple treatments may have an even more profound restorative effect, if applied at the steady state of the preceding treatment. The two major obstacles involved in NTN delivery to the brain with efficient dosage lie in, first, permeating the BBB and, second, ensuring sufficient bioavailability across the entire structure of interest. In the study preceding this one [18], it was shown that both objectives could be achieved with FUS-induced BBB drug delivery in wild-type mice.

In conclusion, our findings show that by targeting the SN and CPU at the early stages of PD, the nigrostriatal pathway is upregulated, thus reinforcing the strong premise of FUS methodology for allowing otherwise BBB-impermeant bioactive molecules to reach the brain parenchyma and treat the compromised neurons. Administration of neurotrophic factors achieved significant increase in the DA phenotypic marker TH that was localized at the level of the downregulated nigrostriatal pathway. Gene therapy and the triple treatment improved neuronal function at both the dendritic and terminal area while the single treatment only upregulated the former.

This study employed direct delivery of neurotrophic proteins as the pharmacological strategy, therefore substituting gene delivery and the associated risks. On the other hand, gene delivery was proven safe and beneficial to the treated brains accounting as a viable alternative to the difficulties associated with multiple treatments. The AAV-GDNF delivery offered the opportunity of investigating physiological changes due to the continuous production of the neurotrophic factor and the longer survival times constituting the second part of this study. Based on these initial findings, FUS-mediated neurotrophic protein delivery may prove pivotal in the effective reversibility of neurodegeneration at the early stages of the disease where motor control symptoms are most prominent. The study also concluded that repeated protein delivery, similar to gene therapy, improves neuronal function along the entire pathway, further demonstrating the clinical relevance of the methodology and the immediate impact on to current clinical PD treatment.



(caption on next page)

Fig. 6. FUS-facilitated AAV-GDNF delivery induced neuronal upregulation in MPTP mice. a. Experimental timeline where MPTP was given first followed by sonication and a 12-week survival period. Behavioral studies were performed 1 week prior to sonication and repeated at the end of the survival period. b. TH staining of the SN region in mice receiving a combination of AAV/FUS treatments ($n = 6-10$). c. TH+ neurons were counted and intra-group comparisons were made. Significantly higher number of TH+ neurons were found on the AAV+/FUS+ side of the brain compared to the contralateral side. d. TH+ dendrite density was calculated and intra-group comparisons were performed. Significantly higher dendrite density was observed on the AAV+/FUS+ side of the brain. e. Immunofluorescent TH staining revealed much more dopaminergic projections on the AAV+/FUS+ side of the brain. Dendritic densities of the SN region were compared across groups and significantly higher dendritic fiber network ($n = 4-5$; $F_{[3, 13]} = 7.514$; $P = 0.0036$) was identified comparing AAV+/FUS+ to the MPTP group. f. TH staining of the striatum illustrates the ameliorated dopaminergic projections on the AAV+/FUS+ hemisphere. Quantitative analysis of the optical density ratio demonstrated significant difference ($n = 4-5$; $F_{[3, 17]} = 4.733$; $P = 0.014$) between the AAV+/FUS+ to the MPTP group. g. Amphetamine-elicited behavioral studies revealed more frequent clockwise (toward the remaining lesion side) rotation, signifying more prominent dopaminergic function on the hemisphere receiving AAV+/FUS+ treatment.

Acknowledgements

This work was supported by the National Institutes of Health (AG038961, EB009041, NS111176, NS099862, NS072428, and NS107442), US Department of Defense Award W81XWH-13-1-0416, the Focused Ultrasound Foundation, the Kavli Institute and the Kinetics Foundation. The authors wish to acknowledge Holly Moore, Ph.D. and Muhammad O. Chohan, M.D. for performing the liquid chromatography as well as Javier Blesa De Los Mozos, Ph.D., Department of Pathology, Columbia University and Ioannis Manousakis, Department of Computer Science, Rutgers University, for his insightful discussions. For the graphical abstract, three-dimensional macromolecular structures of the AAV virus (PDB: 3J1Q, [58]), NTN (PDB: 5NMZ, [59]) and GDNF (PDB: 4VZ4, [60]) proteins were obtained from the Protein Data Bank while the anatomical and functional representation of the nigrostriatal pathway was constructed by MEK with tools provided by Allen Brain Institute.

Authors' contributions

This study was designed by EEK, SP, MEK, SW and GS. The manuscript was written by EEK, SP, VLJ, MEK and SW. Animal experiments were performed by MEK, SW and GS. Cavitation detection and MRI scanning were performed by TS and YH. Behavioral testing, immunohistochemistry, stereological counting and HPLC were performed by TK, OOO and CA. Simulations were carried out and analyzed by HK. Finally, the analysis was carried out by MEK and SW. Additional advice was provided by VLJ and SP.

Disclosure/Conflict of interest

The authors declare no conflicting interests with respect to the research, authorship or publication of the current article.

Additional materials and methods including a summarizing table of the in vivo experiments, the quantification flowchart, higher magnification figures and supporting data are provided in SI Materials and Methods.

Appendix A. Supplementary data

Supplementary data to this article can be found online at <https://doi.org/10.1016/j.jconrel.2019.03.030>.

References

- [1] B.J. Spencer, I.M. Verma, Targeted delivery of proteins across the blood-brain barrier, *Proc. Natl. Acad. Sci. U. S. A.* 104 (18) (2007) 7594–7599.
- [2] J. Stockwell, N. Abdi, X. Lu, O. Maheshwari, C. Taghibiglou, Novel central nervous system drug delivery systems, *Chem. Biol. Drug Des.* 83 (5) (2014) 507–520.
- [3] K. Hynynen, N. McDannold, N. Vykhodtseva, F.A. Jolesz, Noninvasive MR imaging-guided focal opening of the blood-brain barrier in rabbits, *Radiology* 220 (3) (2001) 640–646.
- [4] G. Samiotaki, E.E. Konofagou, Dependence of the reversibility of focused-ultrasound-induced blood-brain barrier opening on pressure and pulse length in vivo, *IEEE Trans. Ultrason. Ferroelectr. Freq. Control* 60 (11) (2013) 2257–2265.
- [5] G. Samiotaki, F. Vlachos, Y.S. Tung, E.E. Konofagou, A quantitative pressure and microbubble-size dependence study of focused ultrasound-induced blood-brain barrier opening reversibility in vivo using MRI, *Magn. Reson. Med.* 67 (3) (2012) 769–777.
- [6] H. Chen, G.Z. Yang, H. Getachew, C. Acosta, C. Sierra Sanchez, E.E. Konofagou, Focused ultrasound-enhanced intranasal brain delivery of brain-derived neurotrophic factor, *Sci. Rep.* 6 (2016) 28599.
- [7] J.F. Jordao, E. Thevenot, K. Markham-Coultes, T. Scarcelli, Y.Q. Weng, K. Xhima, et al., Amyloid-beta plaque reduction, endogenous antibody delivery and glial activation by brain-targeted, transcranial focused ultrasound, *Exp. Neurol.* 248 (2013) 16–29.
- [8] J. Park, M. Aryal, N. Vykhodtseva, Y.Z. Zhang, N. McDannold, Evaluation of permeability, doxorubicin delivery, and drug retention in a rat brain tumor model after ultrasound-induced blood-tumor barrier disruption, *J. Control. Release* 250 (2017) 77–85.
- [9] C.Y. Lin, H.Y. Hsieh, C.M. Chen, S.R. Wu, C.H. Tsai, C.Y. Huang, et al., Non-invasive, neuron-specific gene therapy by focused ultrasound-induced blood-brain barrier opening in Parkinson's disease mouse model, *J. Control. Release* 235 (2016) 72–81.
- [10] C.H. Fan, C.Y. Ting, C.Y. Lin, H.L. Chan, Y.C. Chang, Y.Y. Chen, et al., Noninvasive, targeted, and non-viral ultrasound-mediated GDNF-plasmid delivery for treatment of Parkinson's disease, *Sci. Rep.* 6 (2016) 19579.
- [11] S. Wang, O.O. Olumolade, T. Sun, G. Samiotaki, E.E. Konofagou, Noninvasive, neuron-specific gene therapy can be facilitated by focused ultrasound and recombinant adeno-associated virus, *Gene Ther.* 22 (1) (2015) 104–110.
- [12] A. Carpentier, M. Canney, A. Vignot, V. Reina, K. Beccaria, C. Horodyckid, et al., Clinical trial of blood-brain barrier disruption by pulsed ultrasound, *Sci. Transl. Med.* 8 (343) (2016) 343re2.
- [13] Y. Oiwa, R. Yoshimura, K. Nakai, T. Itakura, Dopaminergic neuroprotection and regeneration by neurturin assessed by using behavioral, biochemical and histochemical measurements in a model of progressive Parkinson's disease, *Brain Res.* 947 (2) (2002) 271–283.
- [14] C. Rosenblad, D. Kirik, B. Devaux, B. Moffat, H.S. Phillips, A. Bjorklund, Protection and regeneration of nigral dopaminergic neurons by neurturin or GDNF in a partial lesion model of Parkinson's disease after administration into the striatum or the lateral ventricle, *Eur. J. Neurosci.* 11 (5) (1999) 1554–1566.
- [15] R. Grondin, Z. Zhang, Y. Ai, F. Ding, A.A. Walton, S.P. Sargener, et al., Intra-putamenal infusion of exogenous neurturin protein restores motor and dopaminergic function in the globus pallidus of MPTP-lesioned rhesus monkeys, *Cell Transplant.* 17 (4) (2008) 373–381.
- [16] N.K. Patel, M. Bunnage, P. Plaha, C.N. Svendsen, P. Heywood, S.S. Gill, Intra-putamenal infusion of glial cell line-derived neurotrophic factor in PD: a two-year outcome study, *Ann. Neurol.* 57 (2) (2005) 298–302.
- [17] J.T. Slevin, G.A. Gerhardt, C.D. Smith, D.M. Gash, R. Kryscio, B. Young, Improvement of bilateral motor functions in patients with Parkinson disease through the unilateral intra-putamenal infusion of glial cell line-derived neurotrophic factor, *J. Neurosurg.* 102 (2) (2005) 216–222.
- [18] R.T. Bartus, T.L. Baumann, J. Siffert, C.D. Herzog, R. Alterman, N. Boulis, et al., Safety/feasibility of targeting the substantia nigra with AAV2-neurturin in Parkinson patients, *Neurology* 80 (18) (2013) 1698–1701.
- [19] J.G. Nutt, K.J. Burchiel, C.L. Comella, J. Jankovic, A.E. Lang, E.R. Laws Jr. et al., Randomized, double-blind trial of glial cell line-derived neurotrophic factor (GDNF) in PD, *Neurology* 60 (1) (2003) 69–73.
- [20] A.E. Lang, S. Gill, N.K. Patel, A. Lozano, J.G. Nutt, R. Penn, et al., Randomized controlled trial of intra-putamenal glial cell line-derived neurotrophic factor infusion in Parkinson disease, *Ann. Neurol.* 59 (3) (2006) 459–466.
- [21] M.F. Salvatore, Y. Ai, B. Fischer, A.M. Zhang, R.C. Grondin, Z. Zhang, et al., Point source concentration of GDNF may explain failure of phase II clinical trial, *Exp. Neurol.* 202 (2) (2006) 497–505.
- [22] B.J. Hoffer, A. Hoffman, K. Bowenkamp, P. Huettl, J. Hudson, D. Martin, et al., Glial cell line-derived neurotrophic factor reverses toxin-induced injury to midbrain dopaminergic neurons in vivo, *Neurosci. Lett.* 182 (1) (1994) 107–111.
- [23] B.A. Horger, M.C. Nishimura, M.P. Armanini, L.C. Wang, K.T. Poulsen, C. Rosenblad, et al., Neurturin exerts potent actions on survival and function of midbrain dopaminergic neurons, *J. Neurosci.* 18 (13) (1998) 4929–4937.
- [24] G. Samiotaki, C. Acosta, S. Wang, E.E. Konofagou, Enhanced delivery and bioactivity of the neurturin neurotrophic factor through focused ultrasound-mediated blood-brain barrier opening in vivo, *J. Cereb. Blood Flow Metab.* 35 (4) (2015) 611–622.
- [25] W. Dauer, S. Przedborski, Parkinson's disease: mechanisms and models, *Neuron* 39 (6) (2003) 889–909.

- [26] U. Ungerstedt, G.W. Arbuthnot, Quantitative recording of rotational behavior in rats after 6-hydroxy-dopamine lesions of the nigrostriatal dopamine system, *Brain Res.* 24 (3) (1970) 485–493.
- [27] G. Mercanti, G. Bazzu, P.A. Giusti, 6-hydroxydopamine in vivo model of Parkinson's disease, *Meth. Mol. Biol.* (Clifton, NJ) 846 (2012) 355–364.
- [28] L.V. Kalia, A.E. Lang, Parkinson's disease, *Lancet* 386 (9996) (2015) 896–912.
- [29] L.S. Ishihara, A. Cheesbrough, C. Brayne, A. Schrag, Estimated life expectancy of Parkinson's patients compared with the UK population, *J. Neurol. Neurosurg. Psychiatry* 78 (12) (2007) 1304–1309.
- [30] T.N. Taylor, J.G. Greene, G.W. Miller, Behavioral phenotyping of mouse models of Parkinson's disease, *Behav. Brain Res.* 211 (1) (2010) 1–10.
- [31] J.A. Feshitan, C.C. Chen, J.J. Kwan, M.A. Borden, Microbubble size isolation by differential centrifugation, *J. Colloid Interface Sci.* 329 (2) (2009) 316–324.
- [32] S. Sirsi, M. Borden, Microbubble compositions, properties and biomedical applications, *Bubble Sci. Eng. Technol.* 1 (1–2) (2009) 3–17.
- [33] J.J. Choi, K. Selert, Z. Gao, G. Samiotaki, B. Baseri, E.E. Konofagou, Noninvasive and localized blood-brain barrier disruption using focused ultrasound can be achieved at short pulse lengths and low pulse repetition frequencies, *J. Cereb. Blood Flow Metab.* 31 (2) (2011) 725–737.
- [34] S. Wang, G. Samiotaki, O. Olumolade, J.A. Feshitan, E.E. Konofagou, Microbubble type and distribution dependence of focused ultrasound-induced blood-brain barrier opening, *Ultrasound Med. Biol.* 40 (1) (2014) 130–137.
- [35] T.D. Mast, Empirical relationships between acoustic parameters in human soft tissues, *Acoust. Res. Lett. Online* 1 (2) (2000) 37–42.
- [36] B.E. Treeby, J. Jaros, A.P. Rendell, B.T. Cox, Modeling nonlinear ultrasound propagation in heterogeneous media with power law absorption using a k-space pseudospectral method, *J. Acoust. Soc. Am.* 131 (6) (2012) 4324–4336.
- [37] H.A. Kamimura, S. Wang, S.Y. Wu, M.E. Karakatsani, C. Acosta, A.A. Carneiro, et al., Chirp- and random-based coded ultrasonic excitation for localized blood-brain barrier opening, *Phys. Med. Biol.* 60 (19) (2015) 7695–7712.
- [38] A.J. Harding, G.M. Halliday, K. Cullen, Practical considerations for the use of the optical disector in estimating neuronal number, *J. Neurosci. Methods* 51 (1) (1994) 83–89.
- [39] M.J. West, L. Slomianka, H.J. Gundersen, Unbiased stereological estimation of the total number of neurons in the subdivisions of the rat hippocampus using the optical fractionator, *Anat. Rec.* 231 (4) (1991) 482–497.
- [40] A.C. Ruifrok, D.A. Johnston, Quantification of histochemical staining by color deconvolution, *Anal. Quant. Cytol. Histol.* 23 (4) (2001) 291–299.
- [41] R.J. Smeyne, C.B. Breckenridge, M. Beck, Y. Jiao, M.T. Butt, J.C. Wolf, et al., Assessment of the effects of MPTP and Paraquat on dopaminergic neurons and microglia in the substantia nigra pars compacta of C57BL/6 mice, *PLoS ONE* 11 (10) (2016) e0164094.
- [42] Z.C. Baquet, D. Williams, J. Brody, R.J. Smeyne, A comparison of model-based (2D) and design-based (3D) stereological methods for estimating cell number in the substantia nigra pars compacta (SNpc) of the C57BL/6J mouse, *Neuroscience* 161 (4) (2009) 1082–1090.
- [43] J.W. Langston, P. Ballard, J.W. Tetrud, I. Irwin, Chronic parkinsonism in humans due to a product of meperidine-analog synthesis, *Science* 219 (4587) (1983) 979–980.
- [44] H. Frielingsdorf, K. Schwarz, P. Brundin, P. Mohapel, No evidence for new dopaminergic neurons in the adult mammalian substantia nigra, *Proc. Natl. Acad. Sci. U. S. A.* 101 (27) (2004) 10177–10182.
- [45] S.B. Rangasamy, K. Soderstrom, R.A. Bakay, J.H. Kordower, Neurotrophic factor therapy for Parkinson's disease, *Prog. Brain Res.* 184 (2010) 237–264.
- [46] P. Hadaczek, L. Johnston, J. Forsayeth, K.S. Bankiewicz, Pharmacokinetics and bioactivity of glial cell line-derived factor (GDNF) and neurturin (NTN) infused into the rat brain, *Neuropharmacology* 58 (7) (2010) 1114–1121.
- [47] V. Jackson-Lewis, S. Przedborski, Protocol for the MPTP mouse model of Parkinson's disease, *Nat. Protoc.* 2 (1) (2007) 141–151.
- [48] N.J. Abbott, Blood-brain barrier structure and function and the challenges for CNS drug delivery, *J. Inher. Metab. Dis.* 36 (3) (2013) 437–449.
- [49] M. Kinoshita, Targeted drug delivery to the brain using focused ultrasound, *Top. Magn. Reson. Imaging* 17 (3) (2006) 209–215.
- [50] F. Marquet, T. Teichert, S.Y. Wu, Y.S. Tung, M. Downs, S. Wang, et al., Real-time, transcranial monitoring of safe blood-brain barrier opening in non-human primates, *PLoS ONE* 9 (2) (2014) e84310.
- [51] N.A. Tatton, S.J. Kish, In situ detection of apoptotic nuclei in the substantia nigra compacta of 1-methyl-4-phenyl-1,2,3,6-tetrahydropyridine-treated mice using terminal deoxynucleotidyl transferase labelling and acridine orange staining, *Neuroscience* 77 (4) (1997) 1037–1048.
- [52] D. Tande, G. Hoglinger, T. Debeir, N. Freundlieb, E.C. Hirsch, C. Francois, New striatal dopamine neurons in MPTP-treated macaques result from a phenotypic shift and not neurogenesis, *Brain* 129 (2006) 1194–1200 Pt 5.
- [53] C. Warren Olanow, R.T. Bartus, T.L. Baumann, S. Factor, N. Boulis, M. Stacy, et al., Gene delivery of neurturin to putamen and substantia nigra in Parkinson disease: a double-blind, randomized, controlled trial, *Ann. Neurol.* 78 (2) (2015) 248–257.
- [54] J.L. Nathanson, Y. Yanagawa, K. Obata, E.M. Callaway, Preferential labeling of inhibitory and excitatory cortical neurons by endogenous tropism of adeno-associated virus and lentivirus vectors, *Neuroscience* 161 (2) (2009) 441–450.
- [55] M. Yaguchi, Y. Ohashi, T. Tsubota, A. Sato, K.W. Koyano, N. Wang, et al., Characterization of the properties of seven promoters in the motor cortex of rats and monkeys after lentiviral vector-mediated gene transfer, *Hum. Gene Ther. Methods* 24 (6) (2013) 333–344.
- [56] P.H. Kelly, D.C. Roberts, Effects of amphetamine and apomorphine on locomotor activity after 6-OHDA and electrolytic lesions of the nucleus accumbens septi, *Pharmacol. Biochem. Behav.* 19 (1) (1983) 137–143.
- [57] Z.I. Kovacs, S. Kim, N. Jikaria, F. Qureshi, B. Milo, B.K. Lewis, et al., Disrupting the blood-brain barrier by focused ultrasound induces sterile inflammation, *Proc. Natl. Acad. Sci. U. S. A.* 114 (1) (2017) E75–E84.
- [58] T.F. Lerch, J.K. O'Donnell, N.L. Meyer, Q. Xie, K.A. Taylor, S.M. Stagg, et al., Structure of AAV-DJ, a retargeted gene therapy vector: cryo-electron microscopy at 4.5 Å resolution, *Structure (London, England: 1993)* 20 (8) (2012) 1310–1320.
- [59] J. Sandmark, G. Dahl, L. Oster, B. Xu, P. Johansson, T. Akerud, et al., Structure and biophysical characterization of the human full-length neurturin-GFRα2 complex: a role for heparan sulfate in signaling, *J. Biol. Chem.* 293 (15) (2018) 5492–5508.
- [60] J.Y. Hsu, S. Crawley, M. Chen, D.A. Ayupova, D.A. Lindhout, J. Higbee, et al., Non-homeostatic body weight regulation through a brainstem-restricted receptor for GDF15, *Nature* 550 (7675) (2017) 255–259.